MULTI-TEMPORAL ANALYSIS IN THE NIGER INLAND DELTA USING ERS 1/2 AND ASAR DATA

Jana Schmidt

Technische Universität Dresden, Department of Geosciences, Mommsenstrasse 13, 01062 Dresden, Germany

ABSTRACT

Due to annual flooding the Niger Inland Delta plays an important role in the Sahel. The flooding influences deciding the land covers inside and in the immediate vicinity of the delta. Using remote sensing technology is an effective way to observe and verify changes in landscape. With its weather and daylight independence Synthetic Aperture Radar (SAR) data emphasize as particularly suitable for large-scaled monitoring. The system parameters of the ERS AMI sensor are quite similar to the available images from the ASAR sensor placed on the environmental satellite ENVISAT. Via four ERS and two ASAR images three change detection methods were performed to analyze which regions are affected by flooding. These areas are the foundation of living (fishery, live stock) for the people in the Inland Delta.

Key words: multi-temporal SAR, change detection, wetland.

1. INTRODUCTION

Using remote sensing technology is an effective way to observe and verify changes in land cover. A decisive advantage of using Synthetic Aperture Radar (SAR) over multispectral sensors is there independence of daylight and weather. Data of multispectral sensors are often influenced by clouds or haze.

The Niger Inland Delta in the Republic of Mali (West Africa) is situated to the south of the Sahara. The Inland Delta is made up of many creeks of the rivers Niger and Bani. The furcations of these creeks are very similar to a delta and represent with mares[1] and mayos[2] a huge alluvium plain. The land cover of the delta is strong affected by annual flooding. In the semi arid West African zone of the Sahel the Inland Delta is vitally important, because it is the foundation of living for many people and animals.

In this paper different ERS and ASAR images of the same area were investigated to find changes in the land cover between the observation dates. Therefor images were analyzed, which were taken in wet and dry season of the years 1992, 1995/96 and 2003/04. Three change detection methods will be applied to the SAR image pairs:

- post-classification,
- image differencing/ratioing and
- principal component analysis.

The suitability of these three methods for detecting changed and unchanges regions respectively is going to investigate.

2. STUDY SITE AND DATA

The studied part of the Niger Inland Delta is situated between the city Mopti in the south and the lakeland area around Lac Débo as northern border of the area of interest. The researched area has an extent of approximately 100 x 100 km. Due to the location to the south of the Sahara local rainfall is very limited during the most time of the year. The studied part is situated between the isohyets of 500 mm in the south and of 250 mm in the north (Fig. 1).

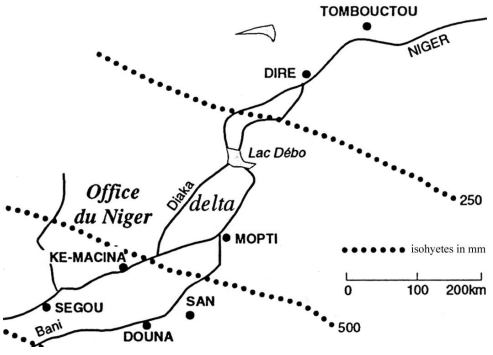

Figure 1. Study site with isohyets, Adapted from [1]

The annual floodings are the result of the rainfall in the catchment areas of the rivers Niger and Bani. Besides

[1] permanent reservoirs
[2] seasonally water-bearing depressions

the variation of the rainfall in the catchment area the dams and reservoirs on the upper stream course influence the inundated area in the Inland Delta directly, which can reach up to 30 000 km^2 [2]. From April to June the study site is characterized by low water and very hot and dry weather [3]. The rainy season starts usually in July, but sometimes the rain begins in June already. The rainy season takes till September and goes along with the increase of the flood. In the time between October and December the flooding will get the maximum water level and starts to decrease. During the flooding and post-flooding period the study site is covered by irrigated fields, grasslands and water bodies mainly. From January till March the water level still decreases and the flooded areas run dry. During this time the green vegetation withers and water bodies become smaller or dry up.

Observations made by the ERS-1 and ERS-2 satellites were done with AMI sensor and ENVISAT images analogous with ASAR. All images were taken in the Image Mode with a VV polarization and an incidence angle at mid swath of approximately 23° on the horizontal earth surface. Both AMI and ASAR sensors are working in C-Band. For the study site these images from different platforms are used (Tab. 1).

Table 1. Acquisition date and platform of the used data with corresponding hydrological moment

date	platform	hydrological moment
1992-06-16	ERS-1	low water
1992-11-03	ERS-1	begin of decreasing water
1995-11-17	ERS-2	begin of decreasing water
1996-04-04	ERS-1	low water
2003-12-05	ENVISAT	begin of decreasing water
2004-03-19	ENVISAT	begin of low water

Because no field data were available of the study site two Medium Resolution Imaging Spectrometer (MERIS) scenes, which were taken at the same time as the ASAR images, are used as reference and interpretation help. By reason of clouds in the MERIS December scene the evaluation is limited. Hence a MERIS image from the 17th December was taken instead. The spatial resolution of MERIS images is of cause quite smaller, but for detecting water bodies, non-flooded and vegetated areas suitable. The MERIS data were atmospheric corrected and resampled. Additionally some Landsat ETM+ and ASTER images from the years 1999/2000 and 2004 were available. Also the descriptions of the land cover of the Niger Inland Delta in [3] were very useful.

Additional, monthly mean water levels of the station Mopti (confluence of Niger and Bani) are made available by the Institut d'Economie Rurale in Bamako/Mopti. The water levels of every year between 1990 and 2004 were available. Fig. 2 shows the flood events in the hydrological years of 1992/93, 1995/96 and 2003/04.

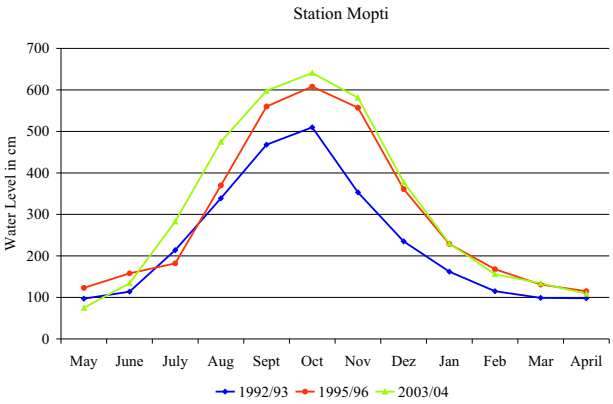

Figure 2. Mean monthly water level of the three hydrological years

Due to no metrological data was available, like rainfall, the observation dates of the images were so selected, that they did not accompanied by the rainy season. Local rainfalls have also influence the land cover during this time of the year. All three wet season images were taken after the maximum water level in the corresponding year. Also for the dry season of 1996 and 2004 images were available. Because no SAR data was available for March and April 1993 respectively, an image taken at the low water season before the flooding period in 1992 was used. But the flooding occurrences of 1991 and 1992 differed not significant from each other, i.e. the course of the graphs are very similar and the annual means differs just about 6 cm. 1991 and 1992 were part of a serial of drier years, which ends in 1994. The graph in Fig. 2 shows that the year of 1992 (blue line) was a dry year comparing to the two other hydrological years.

3. PRE-PROCESSING

Radiometric and geometric calibrations are necessary to accomplish multi-temporal analysis of the available SAR data. The on-board instruments and the processors, which generated the used Precision Image (PRI) products, are sources for radiometric errors which have to be corrected.

3.1. Radiometric Calibration

Through the radiometric calibration the relation between the radar backscattering coefficient σ^0 and the Digital Number (DN) of the pixel is established. Calibrated images can be used for comparing backscatter from different temporal points of observing and from different sensors.

Both ERS-1/-2 and ASAR PRI products are already corrected for antenna elevation gain and range spreading

loss. The radiometric calibration of the DN corresponding to the range and azimuth location (i,j) in ERS-1 and ERS-2 images occur to [4]:

$$A_{ij}^2 = DN_{ij}^2 \cdot \frac{sin\,\alpha_i}{sin\,\alpha_{ref}} \cdot C_i \cdot PowerLoss_{ij} \cdot Factor \quad (1)$$

with

$$Factor = \frac{ProductReplicaPower}{ReferenceReplicaPower} \cdot \frac{1}{K}$$

Only the ERS-1 images must be corrected for replica pulse power variations additionally. Therefore the factor $\frac{ProductReplicaPower}{ReferenceReplicaPower}$ is one for the ERS-2 image. A correction of the Analogue to Digital Convertor (ADC) power loss was not realized, because it affects chiefly large targets with high backscatter coefficients (e.g. large towns) [4]. So the ADC power loss was not considered and the term $PowerLoss_{ij}$ is one as well.

K is a calibration constant and C a correction factor, which depends on the processing center and product processing date. Unfortunately no digital elevation model was available so that assumptions must be made for calculating the local incidence angle α_i. The Niger Inland Delta is on the whole a relative flat terrain, so for the local incidence angles the incidence angles on the ellipsoid were used instead, i.e. no slopes will be considered. The ERS-1 scene from November 1992 is an exception, because this image was generated using a nominal replica pulse. So the calibration was done how described in [4]. Finally the backscatter coefficient for distributed targets can be calculated as follows:

$$\sigma^0 = \frac{1}{N} \cdot \sum A_{ij}^2 \quad (2)$$

For the ASAR PRI images the calculation of σ^0 is more simple, as seen in Eq. 3:

$$\sigma_{ij}^0 = \frac{DN_{ij}^2}{K} \cdot sin\,\alpha_{ij} \quad (3)$$

For further information see [5]. For comparing the backscatter from different dates the dimensionless σ^0 were converted to decibel (dB) on a logarithmic scale for all images.

3.2. Texture Analysis

Calculating the texture parameters is not a pre-processing step. It is mentioned here, because the calculation happens before the next radiometric calibration step: the speckle reduction. The used SAR data are all one-channel images, because of the single polarization mode for PRI images. The similar backscatter behavior of different land covers hinders the classification. With more layers the feature space will be extended, which can improve the classification result. The statistical Gray Level Dependence Method (GLDM) analyzes pixel pairs, whereby a pair consists of a reference and a neighbor pixel [6].

The calculation of the texture parameters happened before the speckle filtering, because due to filtering not only speckle will be removed but also texture information will be reduced as seen in Fig. 3.

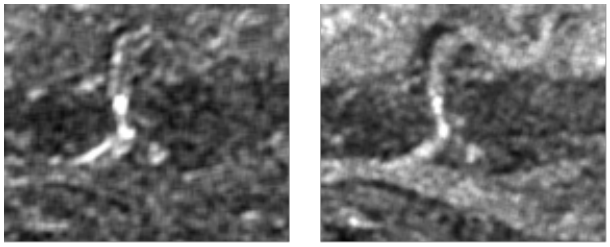

Figure 3. Texture Parameter Dissimilarity calculated from the speckle filtered (left) and non-speckle filtered (right) image

The texture parameters were calculated with different kernel sizes (7 x 7, 11 x 11 and 21 x 21 pixels). The small and large kernel sizes are not suitable for these images. The small kernel size did not capture the large-scaled texture adequate, e.g. the lakes. For the large kernel size (21 x 21 pixels) the image content is too heterogeneous, especially in the flood plain. It contains mixed land cover types, so in the texture calculation too many different land covers are incorporated. Finally calculation of the texture parameters was done with a kernel size of 11 x 11 pixels.

Before suitable texture parameters for the corresponding SAR images were selected, areas of interest (AOI) of different land covers were defined. By the means of this AOI's texture parameters were selected, which might increase the separability of the different AOI's. The parameter Variance and Dissimilarity were chosen for all images. Within the co-occurrence matrix these parameters describe the heterogeneity and the differences between the elements respectively.

3.3. Speckle Reduction

SAR data is influenced by speckle noise, which makes a meaningful classification not possible. The quantitative evaluation of the provided speckle filters in the software ENVI was done by the Equivalent Number of Looks (ENL, Eq. 4) and Normal Mean (NM, Eq. 5) [7]. These two factors were calculated for an as homogeneous as possible test area. The filter should retain the mean and reduce the standard deviation and variance respectively, i.e. the ENL value should be high which indicates reduction of standard deviation. With NM the mean preservation were controlled.

$$ENL = \frac{mean^2}{variance} \quad (4)$$

$$NM = \frac{mean_{filtered}}{mean_{original}} \quad (5)$$

The images were filtered with the quantitative best filter and additionally the edge preservation, sharpness and texture effects were visual controlled. For both ASAR scenes and the four ERS scenes the Gamma MAP filter with a kernel size of 7 x 7 pixel was the most suitable filter.

3.4. Image Co-Registration

For a collectively analysis of the multi-temporal data a precise registration of the images to each other is necessary. A feature of the ASAR PRI products are the geolocation grids with latitude and longitude information, which were used for georeferencing these two images. For the ERS images manual georeferencing were done. At first the images were referenced to topographic map, because in the study site suitable features for georeferencing are difficult to find in SAR data. The geolocation grid for the ASAR images were not as accurate as needed for change detection. Due to afterwards geometric registration between the multi-temporal images were applied.

4. CLASSIFICATION AND MULTI-TEMPORAL ANALYSIS

Supervised classification results are designed as input for post-classification change detection. Classifications were realized, because in opposite to the other two methods a matrix of change information is available. Also image ratioing and principal component analysis (PCA) are techniques, which were successfully applied to study changes in land cover.

4.1. Classification

For a post-classification change detection all images had to be classified by itself. Because for not even one ERS image a multispectral reference images or ground truth data is available Landsat and ASTER images respectively were selected, which were taken under as comparable as possible flooding situations. For visual help at the interpretation of the ERS images, years with similar flooding situations were searched via the course of the mean monthly water levels. These and the two MERIS images were taken for visual comparing and evaluation of the classification results. Due to missing ground truth data it was very important to analyze the given auxiliary date and to detect permanent features (e.g. the fix sand dunes in the north) or features which existence under certain circumstances (like water bodies which are filled during the wet season). These features can be used as AOI's for the maximum likelihood classification.

Especially the ERS image taken during the dry season of the dry year (1992) was difficult to interpret. The central part of the image was low in contrast and the different dark areas were not easy to identify. Through the drought the proportion of vegetation was less, comparing with the other two low water images. So the separation of water and vegetated areas was better than in the other cases. In the majority of cases the water surface is rough through windy conditions. The backscatter were very high and encompass a huge range (e.g. the standard deviation of a profile through the Lac Débo of the low water image of 1996 is around 1.43 dB), which makes the separation of the water areas more difficult. For this reason often areas in the greater lakes, e.g. Lac Débo, were classified as vegetation. Thereby that in the low water period only sparse vegetation exists the water classification was much better.

Visual comparisons of the classified ASAR images with the MERIS data shows in the wet season scenes the separability of the dry (probably rough) regions (e.g. dunes) and flooded areas (which also can include vegetation) is not good enough. It has emerged that flooded areas have been detected, which were classified as dry regions without texture layers. But there were also misclassifications, which influences the post-classification result. The texture layers improved the classification results in many cases, but altogether the qualities of the classification results were not suitable for post-classification change detection. Another disadvantage is the high expenditure of time. Instead methods like image differencing and ratioing as well as principal component analysis were tested.

4.2. Change Detection

The advantages of ratioing over differencing for SAR data are described in [8], so image differencing was excluded. For calculating the ratio image the flooding situation were divided over the corresponding low water situation. Afterwards the ratio images were expressed on a logarithmic scale to uncompress range of variation. This was done for the image pair of 1992 also, so that the decreasing of the backscatter coefficient is uniform displayed with bright gray values and increasing in dark gray values. Light-gray values are near zero and indicates just little backscatter increase or decrease. The bright values mainly show regions, which were former flooded or vegetated and dried out and withered respectively. Dark areas were former flooded and changed to vegetation and regions with soil moisture respectively.

The comparison between the dry year of 1992 and a "normal" one shows in the central part of the Delta huge areas which were not affected by the flooding. Furthermore just

few darker areas are noticeable compared to the other two ratio images. Instead large areas are displayed in light-gray, which indicates just little backscatter changes. One explanation might be the later observation date (in June instead in March/April), but also the fact that the images of 1992 were taken in a dry period plays an important role. It seems that the great lakes, e.g. Lac Débo, were not so strong affected. The reduction of the water surface has the approximately the same dimension as in the other ratio images. But smaller lakes, e.g. Walado Debo, are influenced clearly. A great part of the lake was dry out, but under "normal" conditions the lake is still filled at this time, which shows the right part of Fig. 4. The light-gray values dominate which indicate just small backscatter changes, whereas in the left image dark and bright values prevail.

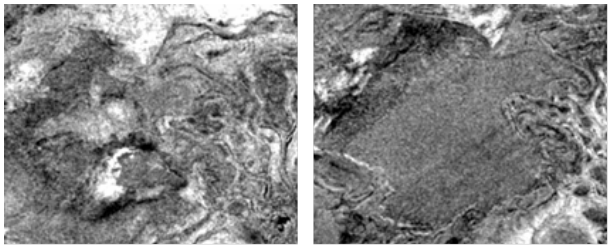

Figure 4. Subset (lake Walado Debo) from ratio images (left 1992, right 1995/1996)

Of course the detection of unchanged areas is quite better than the post-classification, but problems make greater water areas. Because the images were taken under different wind conditions greater water areas have often different backscatter behavior. Although the land cover did not changed the ratio image showing changes and the thresholding (for separating changed and unchanged areas) will be make difficult.

For the purpose that interannual change detection is intended with some more ERS and other SAR images, principal component transformation was applied. The principal component transformation is a linear transformation, which represents multichannel (multidate) input data without correlation [9]. For detecting seasonal and annual changes the image pairs of the dry (1992) and the "normal" (1995/96) years were chosen. The first component (determining through eigenvalue and eigenvector) is placed according to the greatest part of the total variance of the data, the second component to the second largest part and so on. Here the first component contains 81.8%, the second 8.2%, the third 5.8% and the fourth component 4.2% of the variance.

All images have almost the equal contribution to the first component, so it shows common features. The third component mainly shows the differences between the wet season image of the "normal" (1995) and of the dry year (1992). Furthermore the fourth component shows differences between the dry seasons.

Fig 5 is a RGB composite image with the two wet season images and the third principal component. It shows

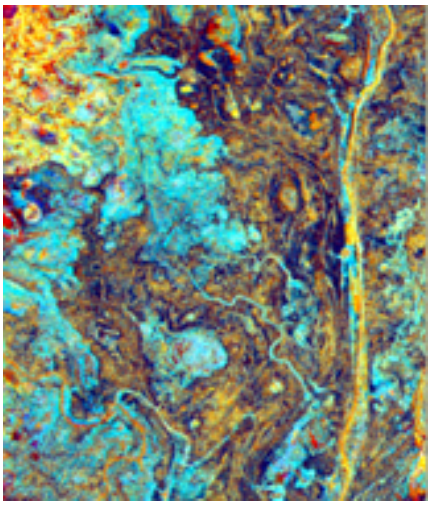

Figure 5. RGB composite image (wet season image of 1992 (red), 1995 (green) and third principal component (blue))

a subset of approximately 17 x 21 km of the study site. The blue areas show the difference of the extent between the flooding in the dry and the "normal" year. The yellow areas are common flooded areas and the brown regions are sand banks. The principal components show dissimilarities between the different dates, but they are difficult to interpret.

5. CONCLUSION AND OUTLOOK

The supervised classification results via maximum likelihood and texture parameters do not create a suitable basis for post-classification and change detection respectively.

By means of image ratioing changes in land cover between two different observation times during a hydrological year can be located. In a next step thresholding (unsupervised) will be performed to outline regions which are non-influenced (unchanged) by the flooding event. Not only between the different images but also within one image the rivers and lakes have huge ranges in the backscatter. So the ratioing image indicates changes, whereas the land cover did not changed. It is to analyze if these features might be detected via the first principal component.

Due to the fact that no elevation model is available especially images taken during the drought years will be interesting, because on this way regions which will be affected at the beginning of the flooding event can be detected. If SAR images were used, which are taken at the regular beginning of the flooding season the land cover maybe already influenced by local rainfall.

It is planned to couple the information about extent with the corresponding water level. The water level at the station Mopti is read every day. Furthermore the water level of the station Akka (in the north of the lakeland area of

Lac Débo) should be considered. Afterwards it is to analyze if the water level (at knowing course of the water level) can be used as suitable indicator to draw conclusions about the extent of the area, which is influenced by the flooding.

ACKNOWLEDGMENTS

The author wishes to thank the European Space Agency for providing the used data.

REFERENCES

[1] Diallo Ousmane Alpha (2000). Contribution à l'étude de la dynamique des écosystèmes des mares dans le Delta Central du Niger, au Mali, Universite Paris I

[2] Zwarts L., Cissé N., Diallo M. (2005). Hydrology of the Upper Niger, pp. 15-41. In: Zwarts L., van Beukering P. Kone B., Wymenga E. (eds.). *The Niger, a lifeline. Effective water management in the Upper Niger Basin.* RIZA, Lelystad / Wetlands International, Sévaré / Institute for Environmental studies (IVM), Amsterdam / A&W ecological consultants, Veenwouden

[3] Mering C., Poncet Y., Hess S., Csaplovics E. (2000). The use of ERS data for monitoring of land cover change in sahelian regions - the example of the delta of the Niger river (Mali), CD ROM Proceedings of the ERS ENVISAT Symposium, Gothenburg

[4] Laur H., Bally P., Meadows, P., Sanchez J., Schaettler B., Lopinto E., Esteban D. (2004). ERS SAR Calibration - Derivation of the backscattering coefficient σ^0 in ESA ERS SAR PRI products, ESA-ESRIN

[5] Rosich B., Meadows P. (2004). Absolute Calibration of ASAR Level 1 Products Generated with PF-ASAR, European Space Agency

[6] Haralick R. M., Shanmugam K., Dinstein I. (1973). Textural Features for Image Classification, *IEEE Transactions on Systems, Man and Cybernetics*, Vol. 3, pp. 610-621

[7] Wang Z., Zhang, J., Wang T. (2004). The Contrast Research of The Methods of Restraining The Speckle Noise of Sar Images, XXth ISPRS Congress, Istanbul, pp. 129-133

[8] Rignot E.J.M., van Zyl J. J. (1993). Change detection techniques for ERS-1 SAR data, *IEEE Transactions on Geoscience and Remote Sensing*, Vol. 31, pp. 896-906

[9] Lillesand T. M., Kiefer R. W., Chipman J. W. (2004). *Remote Sensing and Image Interpretation 5th Edition*, J. Wiley & Sons